Interaction between Soluble P-Selectin and Soluble P-Selectin Glycoprotein Ligand 1: Equilibrium Binding Analysis†

Kevin Croce,‡,§ Steven J. Freedman,‡,|| Barbara C. Furie,⊥ and Bruce Furie*,⊥

Center for Hemostasis and Thrombosis Research, Beth Israel Deaconess Medical Center and Harvard Medical School, Boston, Massachusetts 02215, and the Department of Biochemistry, Tufts University School of Medicine, Boston, Massachusetts 02111

Received June 8, 1998; Revised Manuscript Received September 10, 1998

ABSTRACT: Leukocyte rolling in the vasculature is mediated by the interaction of endothelial P-selectin and leukocyte P-selectin glycoprotein ligand 1 (PSGL-1). Since cell−cell interaction mediated by P-selectin and PSGL-1 is cooperative and complex, we have developed a model system to examine the binding of P-selectin to PSGL-1 in a soluble system. Equilibrium binding analyses were performed with truncated forms of soluble human P-selectin and dimeric PSGL-1, both lacking the transmembrane domain and both produced in Chinese hamster ovary (CHO) cells. Soluble PSGL-1 (sPSGL-1), which contains no tryptophan residues and exhibits no intrinsic fluorescence, was harvested from CHO cells cotransfected with either fucosyltransferase III (sPSGL-1/Fuc-TIII) or fucosyltransferase VII (sPSGL-1/Fuc-TVII). Both fucosylation isoforms of sPSGL-1 bound to sP-selectin. The interaction of sP-selectin and sPSGL-1 was studied by monitoring changes in the intrinsic fluorescence of sP-selectin upon binding to sPSGL-1. Binding of sPSGL-1 to sP-selectin in the presence of calcium caused an increase in tryptophan fluorescence that could be reversed by the addition of ethylenediaminetetraacetic acid (EDTA). The fluorescence enhancement of sP-selectin by sPSGL-1 was used to generate binding isotherms, and these data were fitted to a bimolecular binding model. The binding constant, K_d, for the binding of sPSGL-1/Fuc-TIII and sPSGL-1/Fuc-TVII to sP-selectin was 3 ± 2 nM and 80 ± 44 nM, respectively. Monomeric sP-selectin bound to dimeric sPSGL-1 with a 2:1 stoichiometry. In a system in which both protein species are soluble and lack transmembrane domains, these results indicate high-affinity interaction between P-selectin and PSGL-1. Furthermore, the fucosylation pattern of PSGL-1 can affect its affinity for P-selectin. These binding constants can be used to explore models of cell adhesion in flow systems.

During inflammation, the adhesion of leukocytes to vascular endothelium in flowing blood is controlled by a multistep process involving distinct classes of transmembrane adhesion molecules (*1*, *2*). Initial tethering followed by rolling of leukocytes along the endothelial cell lining of the vessel wall is mediated by members of the selectin family of adhesion molecules and their mucin-like ligands (*3*, *4*). Within this context, the interaction of endothelial P-selectin and leukocyte PSGL-1[1] is required for effective targeting of white blood cells to areas of inflammation (*5*).

P-selectin is a member of the selectin family of adhesion molecules, type I transmembrane proteins whose ligand binding domain includes a C-type lectin domain and an epidermal growth factor (EGF) domain (*6*, *7*). It is constitutively expressed in platelets and endothelial cells, where it is sequestered in the intracellular storage granules of resting cells (*8*−*10*). Cell activation leads to rapid translocation of P-selectin to the cell surface and enables interaction with its counterreceptor PSGL-1 (*8*−*12*). Reflecting participation of a C-type lectin domain, P-selectin ligand recognition is calcium-dependent (*12*−*14*).

PSGL-1, the best-characterized ligand for P-selectin, is a highly glycosylated homodimer found on a number of leukocyte subtypes (*13*, *15*, *16*). It lacks homology with any known protein and requires specific glycosylation, fucosylation, and tyrosine sulfation patterns in order to bind to P-selectin (*13*, *17*−*22*).

The dynamics of the cell−cell adhesion mediated through P-selectin and PSGL-1 in flowing blood are complex. Adhesion is governed by molecular parameters such as the receptor−ligand affinity, receptor−ligand on and off rates, and receptor−ligand densities (*23*, *24*). Additional rheological factors such as the flow rate and viscosity of blood are also of critical importance in determining whether cells will adhere to one another under physiologic conditions in the vasculature (*25*, *26*). To support rolling under the influence of shear force in flowing blood, the P-selectin−

† This work was supported in part by a grant from the National Institutes of Health (HL51926).

* To whom correspondence should be addressed: Research East BIDMC, P.O. Box 15732, Boston, MA 02215.

‡ Tufts University School of Medicine.

§ This work is in partial fulfillment of the requirements for the degree of Doctor of Philosophy from Tufts University.

|| Present address: Department of Medicine, University of California, San Francisco.

⊥ Harvard Medical School and Beth Israel Deaconess Medical Center.

[1] Abbreviations: PSGL-1, P-selectin glycoprotein ligand 1; sPSGL-1, soluble P-selectin glycoprotein ligand 1; sP-selectin, soluble P-selectin; Fuc-TIII, fucosyltransferase III; Fuc-TVII, fucosyltransferase VII; Fuc-TIV, fucosyltransferase IV; PBS, phosphate-buffered saline; TBS, Tris-buffered saline; KLH, keyhole limpet hemocyanin; ELISA, enzyme-linked immunosorbent assay; DTT, dithiothreitol.

10.1021/bi981341g CCC: $15.00
Published on Web 11/04/1998

PSGL-1 bond has been proposed to have high molecular affinity and fast association−dissociation rates (*2*, *27*). To date, the complex nature of cell surfaces had hindered determination of the binding parameters that define P-selectin and PSGL-1 interaction. Equilibrium binding analysis of purified P-selectin to cells generated an apparent dissociation constant of 70 nM but receptor−ligand density on the cell surface, homogeneity of ligand distribution on this surface, and cooperativity of binding complicate interpretation of these data (*28*).

An understanding of the molecular kinetic parameters for adhesion molecule interactions is essential to determining the relative contribution of various receptor pairs to the rolling of leukocytes in the vasculature. The purpose of this study was to determine the affinity of soluble P-selectin for soluble PSGL-1 in a simple, chemically defined system in which the two components could be studied in the solution phase.

MATERIAL AND METHODS

Materials. Cyanogen bromide-activated Sepharose was purchased from Pharmacia (Piscataway, NJ). All other chemicals were ACS grade or better and were obtained from Sigma Chemical Co. (St. Louis, MO).

Recombinant Proteins. Pure, soluble P-selectin (sP-selectin) was purchased from R&D Systems (Minneapolis, MN). This recombinant form of human sP-selectin is produced in Chinese hamster ovary (CHO) cells and contains the N-terminal 730 amino acids of the mature protein. It lacks the transmembrane and cytoplasmic segments. The material eluted as a single peak by fast protein liquid chromatography (FPLC) gel filtration, consistent with the monomeric nature of sP-selectin in solution. The concentration of sP-selectin was determined by amino acid analysis.

Pure soluble P-selectin glycoprotein ligand-1 (sPSGL-1) was a generous gift of Genetics Institute (Andover, MA). sPSGL-1 was produced in CHO DUKX cells by stable cotransfection of the cells with vectors carrying the I316 construct of the cDNA for PSGL-1 terminating at isoleucine 316, core-2-glycosyltransferase cDNA, and either fucosyltransferase III or fucosyltransferase VII cDNA (*13*). sPSGL-1 was purified by ion-exchange chromatography and gel filtration. Fractions containing dimeric sPSGL-1 were used in these studies. The material ran as a single peak by FPLC gel filtration, consistent with the molecular weight for dimeric sPSGL-1. The material produced in cells cotransfected with fucosyltransferase III cDNA is designated sPSGL-1/Fuc-TIII, while that produced in cells cotransfected with fucosyltransferase VII cDNA is designated sPSGL-1/FucT-VII. The concentration of sPSGL-1 was determined by quantitative enzyme-linked immunosorbent assay (ELISA).

Antibodies. The nonblocking monoclonal anti-human P-selectin antibody AC1.2 was prepared as previously described (*12*). For immunoprecipitation experiments, AC1.2 was conjugated to cyanogen bromide-activated Sepharose at a concentration of 500 μg of antibody/mL of Sepharose.

The polyclonal antibody to PSGL-1 was prepared against a peptide representing residues 42−56 of the predicted sequence for human PSGL-1; a cysteine residue was added at the C-terminus (QATEYEYLDYDFLPETEPPGC) (*13*). The peptide was synthesized using FMOC/*N*-methylpyrrolidone chemistry on an Applied Biosystems Model 430A peptide synthesizer. After cleavage and deprotection, the peptide was purified to homogeneity by reverse-phase high-performance liquid chromatography. The peptide was covalently coupled to keyhole limpet hemocyanin (KLH) through the free cysteine, and then the conjugate was injected intradermally (550 μg) in complete Freund's adjuvant into a New Zealand white rabbit (Rockland). Subsequent injections of immunogen (250 μg) were performed weekly for 2 weeks and then monthly thereafter. Anti-peptide antibodies were purified from rabbit immune serum by immunoaffinity chromatography. The serum was applied to a KLH−Sepharose column to remove antibodies against KLH. The serum proteins that failed to bind to KLH−Sepharose were then applied to a PSGL-1 (42−56)−Sepharose column in which the peptide was covalently attached using Sulfo-Link resin (Pierce). Bound antibodies were eluted with 6 M guanidine hydrochloride and dialyzed into PBS.

Immunoprecipitation and Western Blotting. A 200 μL solution of sP-selectin (100 nM) and sPSGL-1 (50 nM) was incubated at 27 °C for 45 min in 20 mM Tris-HCl, pH 7.6, 100 mM NaCl, 0.005% Tween-80, and 1.0 mM $CaCl_2$. Following incubation, samples were immunoprecipitated for 30 min with 25 μL of AC1.2−Sepharose. After removal of the beads by centrifugation, the AC1.2−Sepharose was twice washed with 300 μL of 20 mM Tris-HCl, pH 7.6, 100 mM NaCl, 0.01% Tween-80, and 1.0 mM $CaCl_2$. Washed precipitates were incubated for 3 min at 80 °C in 40 μL of 20 mM Tris, pH 6.8, 16% glycerol, 5% DTT, and 3.2% SDS, and a 30 μL aliquot was applied to an SDS−7.5% polyacrylamide gel. Following electrophoresis, proteins on the gel were transferred to Immobilon-P (Millipore, New Bedford, MA). Immobilon membranes were blocked with 1% nonfat milk for 1 h and then incubated with 4 μg/mL polyclonal anti-PSGL-1 antibody followed by goat anti-rabbit antibody conjugated to horseradish peroxidase. The blot was developed by enhanced chemiluminescence.

Production of Monomeric sPSGL-1. Dimeric sPSGL-1/Fuc-TVII was reduced and alkylated to produce stable sPSGL-1 monomer by a standard protocol (*29*). To reduce the disulfide bonds, 300 μL of sPSGL-1 (363 μg) was incubated for 2 h at 27 °C with 38 μL of 10% tributylphosphine (final concentration 50 mM) dissolved in 2-propanol. Following incubation, the free cysteines were alkylated through the addition of 4.5 μL of 1 M iodoacetic acid (final concentration 13 mM) in 1 M NaOH. After incubation for 45 min., the protein was dialyzed overnight at 4 °C against 4 L of PBS. Immunoprecipitation experiments with this material were carried out as described above.

Fluorescence Measurements. Fluorescence data were collected with an SLM 8000C fluorescence spectrophotometer. The sP-selectin contained in a 1 × 1 cm fluorescence cuvette was irradiated at 280 nm (slit width 4 nm) and the fluorescence emission was recorded at 340 nm (slit width 8 nm). Measurements were obtained with a 5 s integration. In titration experiments, aliquots of sPSGL-1 (2.4 μM) were added to a 2.5 mL sample of sP-selectin in Tris-buffered saline (TBS) (20 mM Tris-HCl, pH 7.6, 100 mM NaCl, and 0.001% Tween 80) containing 1 mM $CaCl_2$ or 1 mM EDTA. sP-selectin concentrations were 20 and 120 nM for titrations with sPSGL-1/Fuc-TIII or sPSGL-1/Fuc-TVII, respectively. At each titration point, the samples were allowed to

equilibrate for 1.5 min prior to fluorescence measurement. Fluorescence measurements at each point were acquired for 2 min. The excitation shutter was closed between each titration in order to minimize photobleaching. The data are presented as total concentration of sP-selectin binding sites on sPSGL-1 versus $[(F - F_0)/F_0] \times 100$, where F_0 is baseline sP-selectin fluorescence in the absence of sPSGL-1 and F is sP-selectin fluorescence at the corresponding concentration of sPSGL-1. Fluorescence measurements performed in the presence of EDTA were subtracted from those made in the presence of $CaCl_2$ to correct for dilution and minimal fluorescence contributed by sPSGL-1.

Determination of the Equilibrium Binding Constant. The interaction between sP-selectin receptor and sPSGL-1 ligand was modeled as a simple bimolecular equilibrium with a stoichiometry of 1:1

$$\mathrm{R{\cdot}L} \overset{K_d}{\rightleftharpoons} \mathrm{R} + \mathrm{L}$$

where R and L represent free receptor and free ligand, respectively; R·L represents the receptor−ligand complex; and K_d is the dissociation constant describing the interaction between receptor and ligand.

The equation can be written as a function of the dissociation constant, K_d

$$K_d = \frac{[\mathrm{R}][\mathrm{L}]}{[\mathrm{R{\cdot}L}]} \quad (1)$$

where [R] is the concentration of free sP-selectin, [L] is the concentration of free sPSGL-1, and [R·L] is the concentration of the complex at equilibrium. The free concentrations of R and L can be described by

$$[\mathrm{R}] = [\mathrm{R_T}] - [\mathrm{R{\cdot}L}] \quad (2)$$

$$[\mathrm{L}] = [\mathrm{L_T}] - [\mathrm{R{\cdot}L}] \quad (3)$$

$[R_T]$ and $[L_T]$ represent the concentrations of total receptor and total ligand, respectively. Substituting for free receptor and free ligand and solving for the receptor−ligand complex yields

$$[\mathrm{R{\cdot}L}] = [([\mathrm{R_T}] + [\mathrm{L_T}] + K_d) \pm \sqrt{([\mathrm{R_T}] + [\mathrm{L_T}] + K_d)^2 - (4[\mathrm{R_T}][\mathrm{L_T}])}]/2 \quad (4)$$

in which only the subtraction operation can provide meaningful results.

The following equation relates fluorescence measurements to the simple bimolecular equilibrium model outlined above:

$$\frac{F_i}{F_s} = \frac{[\mathrm{R{\cdot}L}]_i}{[\mathrm{R{\cdot}L}]_s} = \frac{[\mathrm{R{\cdot}L}]}{[\mathrm{R_T}]} \quad (5)$$

or after rearrangement,

$$F_i = \frac{F_s[\mathrm{R{\cdot}L}]}{[\mathrm{R_T}]} \quad (6)$$

where F_i is the fluorescence change of sP-selectin produced by the binding of increasing quantities, i, of sPSGL-1. F_s is the fluorescence change of sP-selectin at saturation. $[R{\cdot}L]_i$ is the concentration of receptor−ligand complex as varying quantities, i, of sPSGL-1 are added to a constant amount of sP-selectin, and $[R{\cdot}L]_s$ is the concentration of receptor−ligand complex at saturation of sP-selectin. Substituting eq 4 into eq 6, thus, yields the final equation

$$F_i = \{F_s[([\mathrm{R_T}] + [\mathrm{L_T}] + K_d) \pm \sqrt{([\mathrm{R_T}] + [\mathrm{L_T}] = K_d)^2 - (4[\mathrm{R_T}][\mathrm{L_T}])}]\}/2[\mathrm{R_T}] \quad (7)$$

This relationship is analogous to the model used to evaluate factor VIII binding to phospholipid vesicles (*30*).

The parameters F_s, and K_d, were calculated by a best-fit analysis of the data using eq 7 and the curve-fitting function in Sigma Plot for Windows version 4.0 (SPSS, Chicago, IL). The Sigma Plot curve-fitter uses the Marquardt−Levenberg algorithm to find the coefficients of the independent variable that gives the best fit between the equation and the data. Quality of fit was assessed by convergence of best-fit parameter values when higher or lower initial parameters were used and by visual examination of the residuals to the fitted line.

RESULTS

Characterization of Soluble PSGL-1 and Soluble P-Selectin. Production of functional recombinant soluble PSGL-1 requires cotransfection with the cDNAs for three components: the PSGL-1 I316 construct, core-2-glycosyltransferase, and fucosyltransferase III or VII (*13*). The PSGL-1 I316 construct encodes the N-terminal 275 amino acids of mature PSGL-1 beginning with the furin/PACE cleavage site at residue 41 and ending with the first eight amino acids of the putative transmembrane domain at isoleucine 316. sPSGL-1 lacks the majority of the transmembrane domain and the entire cytoplasmic tail of full-length PSGL-1. Its amino acid sequence contains no tryptophans and it retains one of three original cysteines near the C-terminal end of the molecule (Figure 1). sPSGL-1 used for these studies was produced in stably transfected CHO cells cotransfected with core-2-glycosyltransferase and either fucosyltransferase III or VII. Both fucosylation isoforms were utilized in our studies and are denoted as sPSGL-1/Fuc-TIII or sPSGL-1/Fuc-TVII.

Because wild-type PSGL-1 exists as a disulfide-linked homodimer on the surface of neutrophils and monocytes (*16*, *31*), we determined whether sPSGL-1 is monomeric or dimeric. Purified sPSGL-1/Fuc-TIII or Fuc-TVII was subjected to electrophoresis on SDS−polyacrylamide gels and blotted with a polyclonal anti-human-PSGL-1 antibody (Figure 2A). Samples run in the presence of reducing agent migrated as monomers with molecular weights of 113 000 and 116 000 for sPSGL-1/Fuc-TIII and sPSGL-1/Fuc-TVII, respectively. In the absence of reducing agent, greater than 95% of both sPSGL-1 species existed as dimers. These results demonstrate that sPSGL-1 homodimerizes through an intermolecular disulfide bond between cysteines located at position 310. The difference in electrophoretic mobility observed for the sPSGL-1/Fuc-TIII and sPSGL-1/Fuc-TVII isoforms are likely due to differences in the extent of their fucosylation or in their fucosylation patterns. When subjected to gel filtration, the sPSGL-1/Fuc-TIII and sPSGL-1/Fuc-TVII used in these studies chromatographed as single

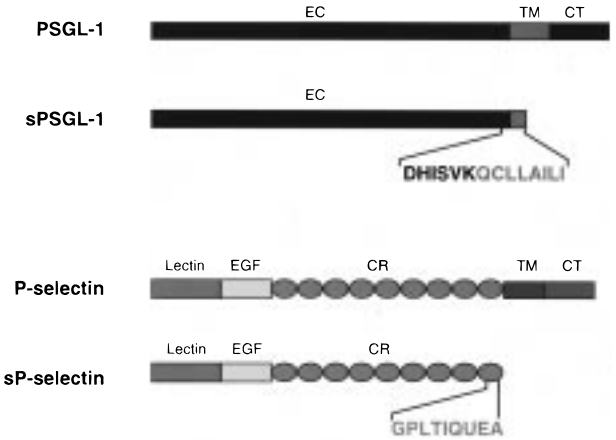

FIGURE 1: Recombinant soluble PSGL-1 and soluble P-selectin. sPSGL-1 was produced in CHO cells cotransfected with cDNA for the PSGL-1 I316 construct, core-2-glycosyltransferase, and fucosyltransferase III or fucosyltransferase VII. sPSGL-1 terminates eight residues within the transmembrane domain at isoleucine 316; it contains one cysteine and no tryptophans. sPSGL-1 has all of the posttranslational modifications necessary for binding to P-selectin. EC, extracellular region; TM, transmembrane region; CT, cytoplasmic tail. The C-terminal residues are shown in the one-letter code for amino acids. sP-selectin is also produced in CHO cells through stable transfection. sP-selectin contains the N-terminal 730 amino acids of P-selectin, truncating at alanine 771 just proximal to the transmembrane domain. It has 17 tryptophan residues available for measurement of intrinsic protein fluorescence. EGF, epidermal growth factor domain; CR, consensus repeat domain. The C-terminal residues of sP-selectin are shown in the one-letter code for amino acids.

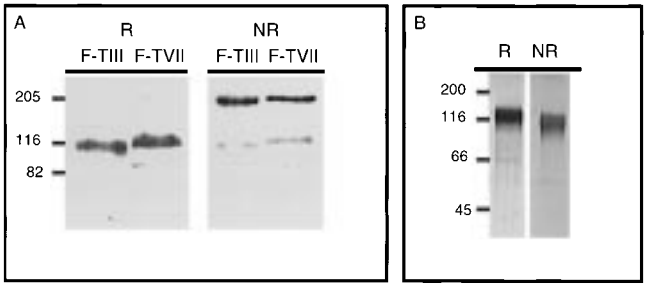

FIGURE 2: Analysis of sPSGL-1 and sP-selectin by SDS−polyacrylamide gel electrophoresis. (A) Pure sPSGL-1/Fuc-TIII and sPSGL-1/Fuc-TVII were subjected to electrophoresis on SDS−polyacrylamide gels and blotted with polyclonal anti-human-PSGL-1 antibody. (B) Pure sP-selectin was subjected to electrophoresis on SDS−polyacrylamide gels and protein was visualized by silver staining. R, in the presence of DTT; NR, in the absence of DTT.

homogeneous peaks consistent with a molecular weight of about 200 000. This is consistent with the dimeric form. No evidence of formation of higher molecular weight species was observed.

The sP-selectin construct encodes the lectin, EGF, and consensus repeat domains and is truncated at alanine 771, just proximal to the transmembrane domain (Figure 1). It contains 17 tryptophan residues which are useful fluorophores for measurement of intrinsic fluorescence. sP-selectin eluted as a homogeneous peak when subjected to FPLC gel filtration.

To confirm that sP-selectin does not dimerize through disulfide bonds, sP-selectin was subjected to electrophoresis on SDS−polyacrylamide gels and proteins were visualized by silver staining (Figure 2B). Samples run in the presence and absence of reducing agent migrated as monomers with molecular weights of 116 000 and 111 000 respectively, demonstrating that sP-selectin is not a dimer. sP-selectin has previously been shown to be an extended rod-shaped monomer in solution (*28*).

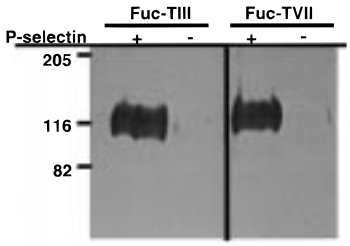

FIGURE 3: Precipitation of dimeric sPSGL-1 by sP-selectin. sP-selectin and dimeric sPSGL-1 (+) or sPSGL-1 alone (−) were incubated for 30 min in the presence of 1 mM calcium. After incubation, the samples were immunoprecipitated with the non-function-blocking anti-P-selectin monoclonal antibody AC1.2 bound to Sepharose. Immunoprecipitated proteins were eluted from the antibody-coated Sepharose by denaturation with gel loading buffer containing DTT and subjected to electrophoresis and Western blotting with anti-PSGL-1 polyclonal antibody.

Direct Binding Studies of Dimeric sPSGL-1 and sP-Selectin. The direct binding of sP-selectin to sPSGL-1 in solution was assessed by immunoprecipitation experiments. Samples containing 50 nM dimeric sPSGL-1/Fuc-TIII or sPSGL-1/Fuc-TVII were incubated in the presence or the absence of 100 nM sP-selectin and protein complexes were precipitated with the nonblocking monoclonal anti-P-selectin antibody AC1.2 conjugated to Sepharose. This antibody does not inhibit P-selectin−receptor interaction (*12*). Proteins in the immunopreciptates were separated by electrophoresis under reducing conditions and detected by Western blot with purified polyclonal anti-PSGL-1 antibody. sPSGL-1 was precipitated by AC1.2 in the presence but not in the absence of P-selectin (Figure 3). As expected, sPSGL-1 binding to sP-selectin was dependent on the presence of calcium (data not shown). This experiment demonstrates that the soluble recombinant forms of P-selectin and PSGL-1 bind effectively in solution.

Direct Binding Studies of Monomeric and Dimeric sPSGL-1 and sP-Selectin. Reduction and alkylation of sPSGL-1 was performed in order to prevent dimerization through the intermolecular disulfide bond occurring between the single cysteine in the molecule at residue 310. Reduced and alkylated sPSGL-1 subjected to electrophoresis and immunoblotting with anti-human-PSGL-1 antibody in the absence of reducing agents migrated with a molecular weight of 116 000, demonstrating that it is predominantly a monomer (Figure 4). The 5% dimeric sPSGL-1 remaining in this sample is seen as a minor component migrating at a molecular weight of approximately 205 000. Reduced and alkylated sPSGL-1/Fuc-TVII was then assayed for its ability to bind to sP-selectin by the coimmunoprecipitation procedure outlined in the experiments depicted in Figure 3. Reduced and alkylated sPSGL-1/Fuc-TVII (100 nM) was incubated in the presence or the absence of 100 nM sP-selectin and protein complexes were precipitated with the nonblocking monoclonal anti-P-selectin antibody AC1.2 conjugated to Sepharose. Immunoprecipitated proteins were then separated under nonreducing conditions and detected by Western blot with purified anti-PSGL-1 antibody. Mon-

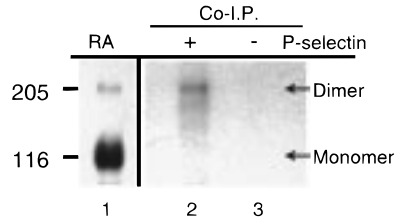

FIGURE 4: Production of monomeric sPSGL-1 and binding of monomeric and dimeric sPSGL-1 to sP-selectin. A western blot of reduced and alkylated sPSGL-1/Fuc-TVII is shown in lane 1. The dominant species is monomeric sPSGL-1 but some dimer sPSGL-1 is observed. sP-selectin and reduced and alkylated sPSGL-1/Fuc-TVII (+) or reduced and alkylated sPSGL-1 alone (−) were incubated for 30 min in the presence of 1 mM calcium. After incubation, the samples were immunoprecipitated with the non-blocking anti-P-selectin monoclonal antibody AC1.2 bound to Sepharose. Immunoprecipitated proteins were eluted from the antibody-coated Sepharose by denaturation with nonreducing gel loading buffer and subjected to electrophoresis and Western blotting with anti-PSGL-1 polyclonal antibody (lanes 2 and 3). RA, reduced and alkylated.

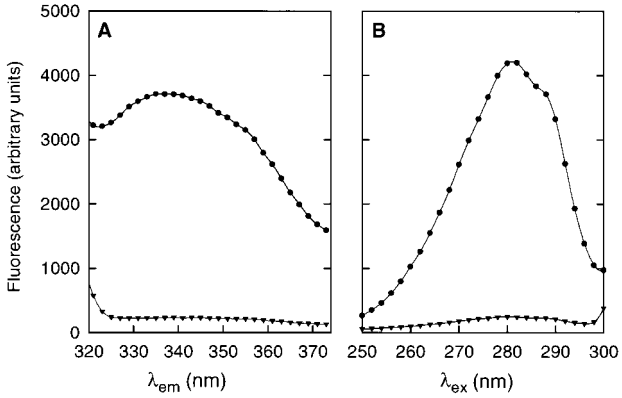

FIGURE 5: Fluorescence emission and excitation spectra of sP-selectin and sPSGL-1/Fuc-TIII. Fluorescence spectra were collected on 100 nM samples of sP-selectin (●) and 50 nM dimeric sPSGL-1/Fuc-TIII (▼). (A) sP-selectin and sPSGL-1/Fuc-TIII were excited at 280 nm. Emission was measured from 320 to 375 nM. (B) sP-selectin and sPSGL-1 were excited between 250 and 300 nm and emission was monitored at 340 nm.

omeric sPSGL-1/Fuc-TVII was not precipitated by P-selectin under these conditions (Figure 4). The minor dimeric fraction of sPSGL-1 did, however, bind to sP-selectin, suggesting its divalent status is important for binding to sP-selectin.

Fluorescence Emission and Excitation Profiles of sPSGL-1. To develop an equilibrium binding assay for the interaction of sPSGL-1 and sP-selectin, we examined the fluorescent properties of these molecules. Fluorescence spectra were obtained on a 50 nM sample of dimeric sPSGL-1/Fuc-TIII. sPSGL-1/Fuc-TIII showed no fluorescence emission between 320 and 375 nm when protein was irradiated at 280 nm (Figure 5A). The excitation spectrum of sPSGL-1/Fuc-TIII also showed no fluorescence at 340 nm when the protein was excited between 250 and 300 nm (Figure 5B). This lack of fluorescence is consistent with the absence of tryptophan residues in sPSGL-1. The addition of EDTA had no effect on the emission or excitation spectra of sPSGL-1. The fluorescence emission and excitation spectra of sPSGL-1/Fuc-TVII were identical to those of sPSGL-1/Fuc-TIII.

Fluorescence Emission and Excitation Profiles of sP-Selectin. Fluorescence emission and excitation spectra were collected on 100 nM samples of sP-selectin. Irradiation of sP-selectin at 280 nm yielded an emission spectrum with maximum intensity at 340 nm (Figure 5A). The excitation spectrum of sP-selectin was maximal at 280 nm when fluorescence emission was monitored at 340 nm (Figure 5B). sP-selectin solutions containing 1 mM EDTA versus 1 mM $CaCl_2$ had similar emission and excitation spectra, showing a minimal 1−2 nm blue shift and less than 1% difference in the emission intensity between the samples containing 1 mM calcium and 1 mM EDTA. The effect of dilution on the sP-selectin fluorescence signal by the addition of buffer was linear. A correction was made for the effect of dilution on fluorescence during titration.

Fluorescence Enhancement of sP-Selectin upon Binding to sPSGL-1. Because sPSGL-1 showed no intrinsic fluorescence while sP-selectin yields typical protein intrinsic fluorescence, we explored whether changes in the intrinsic fluorescence of sP-selectin occur upon binding of sPSGL-1. Addition of 50 nM dimeric sPSGL-1/Fuc-TIII to a 100 nM solution of sP-selectin in 1 mM $CaCl_2$ led to a 7% increase in sP-selectin fluorescence at 340 nm (Figure 6A). A sPSGL-1 concentration of 75 nM was associated with an additional 3% enhancement in sP-selectin fluorescence attributed to binding of sPSGL-1 to sP-selectin (Figure 6B). The enhancement of sP-selectin fluorescence was saturable at high concentrations of sPSGL-1 (see below). The addition of EDTA reversed the fluorescence enhancement, demonstrating the dependence of this increased sP-selectin fluorescence on its calcium-dependent interaction with sPSGL-1 (Figure 6C). Taken together, these data demonstrate that sP-selectin undergoes an increase in intrinsic fluorescence upon calcium-dependent binding to sPSGL-1. The emission maximum was detected at 340 nm. Binding of sPSGL-1/Fuc-TVII to sP-selectin also resulted in increased sP-selectin fluorescence in similar assays (see below).

Determination of the Equilibrium Binding Affinity of sP-Selectin for sPSGL-1. The enhancement of sP-selectin fluorescence upon binding to sPSGL-1 was used to monitor the interaction of the two proteins. In equilibrium binding experiments, increasing amounts of dimeric sPSGL-1/Fuc-TIII or sPS6L-1/Fuc-TVII were added to a cuvette containing sP-selectin in TBS and 1 mM $CaCl_2$ and the fluorescence was monitored. Equivalent titration experiments were performed in 1 mM EDTA and the fluorescence values were subtracted from the fluorescence observed at the same sPSGL-1 concentration in the presence of calcium to correct for dilution and minor fluorescence of sPSGL-1. The fluorescence change of sP-selectin upon binding to sPSGL-1 was plotted as $[(F - F_0)/F_0)] \times 100$, where F_0 is initial sP-selectin fluorescence and F is sP-selectin fluorescence in the presence of various concentrations of sPSGL-1. The intrinsic fluorescence enhancement of sP-selectin upon binding to sPSGL-1 was used to determine the equilibrium binding constant (K_d) for the association of sP-selectin and sPSGL-1 (Figure 7). Binding data were fit to a bimolecular model for receptor−ligand binding as described in Materials and Methods, where each dimeric PSGL-1 molecule was assumed to have two identical and noninteracting sites for the binding of sP-selectin.

The data in Figure 7A are representative of a series of three experiments for sP-selectin (20 nM) binding to dimeric sPSGL-1/Fuc-TIII. In these experiments the mean K_d for

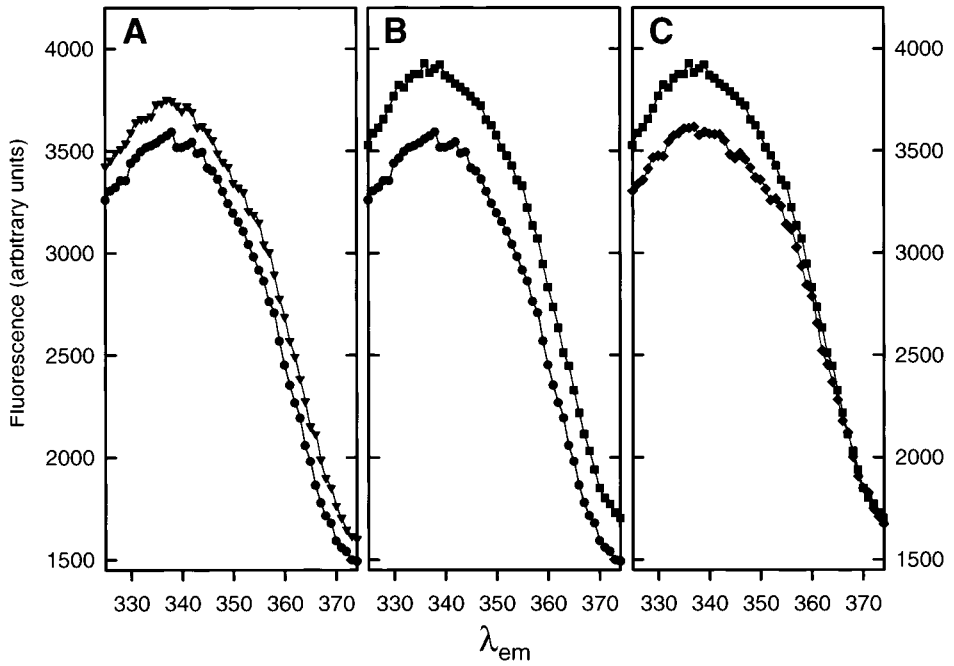

FIGURE 6: Enhancement of intrinsic sP-selectin fluorescence upon binding to sPSGL-1. The fluorescence emission spectrum of sP-selectin was determined in the absence and presence of sPSGL-1 with an excitation wavelength of 280 nm. (A) 100 nM sP-selectin and 1 mM $CaCl_2$ (●); 100 nM sP-selectin, 50 nM dimeric sPSGL-1/Fuc-TIII, and 1 mM $CaCl_2$ (▼). (B) 100 nM sP-selectin and 1 mM $CaCl_2$ (●); 100 nM sP-selectin, 75 nM dimeric sPSGL-1/Fuc-TIII, and 1 mM $CaCl_2$ (■). (C) 100 nM sP-selectin, 75 nM dimeric sPSGL-1/Fuc-TIII, and 1 mM $CaCl_2$ (■); 100 nM sP-selectin, 75 nM dimeric sPSGL-1/Fuc-TIII, 1 mM CaCl, and 5 mM EDTA (◆).

sPSGL-1/Fuc-TIII binding to sP-selectin was 3 ± 2 nM (Table 1). sPSGL-1/Fuc-TVII demonstrated somewhat weaker affinity for sP-selectin. Figure 7B is a typical isotherm for the binding of sPSGL-1/Fuc-TVII to sP-selectin (120 nM). The mean K_d for the binding of dimeric sPSGL-1/Fuc-TVII to sP-selectin was 80 ± 44 nM in three experiments (Table 1). Data from the binding isotherms fit the bimolecular model with greater than 95% confidence in all experiments. A graphical method was used to estimate the stoichiometry of binding of sPSGL-1/Fuc-TIII with sP-selectin in which the fractional fluorescence saturation of sP-selectin enhancement is plotted as a function of the ratio of sPSGL-1 dimer to sP-selectin (*32*). Parallels to the curve are drawn in the linear portion and at saturation. The intersection of these two parallels denotes the stoichiometry of the interaction when a perpendicular is drawn to the *x* axis. Via this method, two sP-selectin molecules bind one sPSGL-1 dimer. Insufficient sPSGL-1/Fuc-TVII was available to accurately estimate its stoichiometry of binding to sP-selectin. Because of the difficulty in assessing the extent of posttranslational modification of each PSGL-1 dimer pair, it is possible that the recombinant material used in these experiments was less than 100% active, in which case the measured affinities might be underestimated. For the same reason we must also be cautious when interpreting the differences between the measured binding affinities of sPSGL-1/Fuc-TIII and Fuc-TVII for sP-selectin as the extent of glycan modification of each isoform was not determined directly.

DISCUSSION

Cell adhesion mediated by reversible interaction between cell surfaces is dependent on the length and flexibility of bonds, density and localization of receptors, and the affinity and kinetic parameters for bond association/dissociation (*33*). Adhesion of leukocytes to the endothelium in the vasculature is also influenced by the rheology of flowing blood, which places shear force on cells as they adhere to the blood vessel wall (*26*). Over the past decade, there have been significant advancements in the identification and characterization of the molecules responsible for leukocyte rolling and adhesion (*7*, *34*, *35*). However, our understanding of the biophysical parameters mediating the binding of these molecules is still very limited since most work has been performed in cellular systems. Measurement of protein−protein affinities, lifetimes, and strain responses of specific receptor−ligand bonds will allow further development of the current models for leukocyte−endothelial adhesion under flow conditions.

The interaction of PSGL-1 and P-selectin is important for leukocyte homing in normal inflammatory and pathological processes (*36*−*40*). Previous attempts to determine the affinity of P-selectin for PSGL-1 utilized equilibrium binding studies on the surfaces of cells where receptor−ligand density and localization and cell surface avidity issues complicate interpretation of the affinity values. An apparent K_d of 70 nM was determined for P-selectin binding to HL60 cells (*28*). To circumvent the complexities of cellular systems, we examined the interaction of soluble P-selectin and soluble PSGL-1 in solution.

The recombinant forms of P-selectin and PSGL-1 utilized are soluble products of transfected cells that lack the transmembrane and cytoplasmic portions of these proteins but contain the complete extracellular regions of the proteins and all of the posttranslational modifications necessary for receptor−ligand binding. The deleted portions of P-selectin and PSGL-1 are not required for functional binding as demonstrated in a number of different assay systems (*19*, *23*, *41*). Similar to wild-type PSGL-1, the sPSGL-1 used in

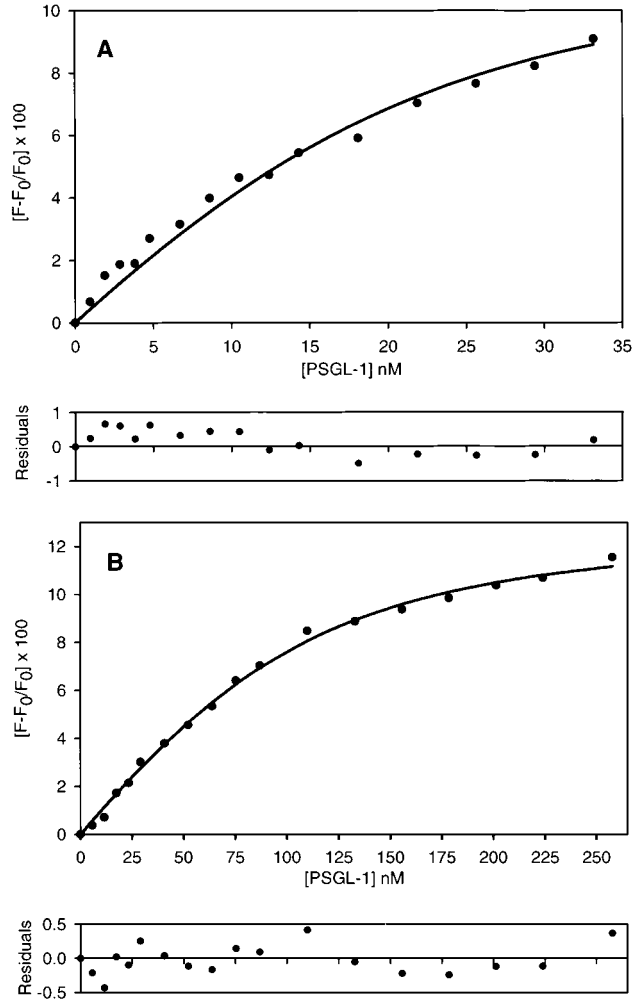

FIGURE 7: sP-selectin/sPSGL-1 binding isotherms. The percent fluorescence enhancement of sP-selectin upon binding to sPSGL-1 is plotted as a function of increasing concentration of sPSGL-1. In these experiments, each molecule of dimeric PSGL-1 was assumed to have two identical and independent sites for the binding of P-selectin. The concentration of sPSGL-1 on the *x*-axis indicates the concentration of total sPSGL-1 binding sites for sP-selectin. The data from the above isotherms were fit to a model for bimolecular binding. In all experiments, the data fit this model with an *R* value demonstrating greater than 95% confidence. The equilibrium binding constants, K_d, for the binding of sP-selectin to sPSGL-1/Fuc-TIII (panel A; Table 1, column 2, experiment 3) and sPSGL-1/Fuc-TVII (panel B; Table 1, column 3, experiment 1) were 3 nM and 80 nM, respectively.

Table 1. Affinity of sPSGL-1 Fuc-TIII and Fuc-TVII for sP-Selectin

	K_d (nM)	
exp	sPSGL-1 Fuc-TIII	sPSGL-1 Fuc-TVII
1	1	32
2	2	70
3	7	140
mean	3 ± 2	80 ± 44

this assay was greater than 95% homodimer as determined by electrophoresis and western blotting. The site of sPSGL-1 dimerization occurs at cysteine 310 as it is the only cysteine found in this soluble form of the molecule.

It is well-established that PSGL-1 requires sialylated, fucosylated O-linked glycans and tyrosine sulfate to bind P-selectin (*13*, *17*−*22*, *42*). O-Linked glycosylation of PSGL-1 depends on the core-2-glycosyltransferase, C2GnT, which is essential for the production of Galβ1−3(Galβ1−4GlcNAcβ1−6)GalNAcα1 on serine or threonine residues (*43*). Fucosylation of these O-linked carbohydrates to create functional PSGL-1 can be accomplished by the α-1,3-fucosyltransferases, fucosyltransferase III or fucosyltransferase VII (*19*).

Even though fucosyltransferase III can be used to create functional sPSGL-1 in recombinant systems fucosyltransferase VII is considered to be the major enzyme that modifies PSGL-1 in vivo in myeloid cells. This fact is further confirmed by murine gene deletion studies in which Fuc-TVII-deficient mice show defects in leukocyte adhesion to all members of the selectin family (*17*). More recent studies have suggested an additional role for fucosyltransferase IV (Fuc-TIV) and Fuc-TVII in the comodification of carbohydrates to produce functional E-selectin ligands (*44*, *45*). The specifics of whether Fuc-TIV and Fuc-TVII cooperate to produce PSGL-1 species that bind to E-selectin have not been determined.

In recombinant systems, fucosyltransferase III and fucosyltransferase VII are able to produce sialyl Lewis x [sLe(x)] epitopes on transfected cells. However, the biochemical activities of these two enzymes have not been fully characterized. Transfection studies in HeLa cells suggest that fucosyltransferase III and fucosyltransferase VII have distinct carbohydrate substrate specificities but the identity of their respective substrates and their exact sites of fucosylation have not been identified (*46*). The differential mobility of PSGL-1/Fuc-TIII and Fuc-TVII by SDS−PAGE suggests that fucosyltransferase III and VII enzymes modify PSGL-1 glycans with differing specificity or to varying extents. Both fucosyl isoforms of sPSGL-1 (Fuc-TIII and Fuc-TVII) bound to sP-selectin.

In direct binding studies only dimeric sPSGL-1 bound with an affinity high enough to support coimmunprecipitation. We have not ruled out the prospect that monomeric sPSGL-1 binds to sP-selectin with low affinity. However, we have been unable to produce enough monomeric sPSGL-1 to formally test this in our direct binding or fluorescence assay. The importance of the dimerization of PSGL-1 in binding to P-selectin has also been demonstrated in a recombinant system where mutated monomeric PSGL-1 expressed on transfected cells failed to bind to P-selectin under static conditions and under physiologic flow conditions (*47*).

PSGL-1, which lacks tryptophans, was not fluorescent when excited at 280 nm. Since sPSGL-1 is transparent in this system, this allowed us to monitor sP-selectin fluorescence as a function of PSGL-1 binding without the complexity of determining alterations in fluorescence of both protein species. The functional binding unit for P-selectin is contained solely within the lectin and EGF domains (*23*, *41*). The lectin domain of P-selectin contains seven of the 17 tryptophans in the molecule, so that 41% of these residues lie within the domain of the protein that interacts directly with PSGL-1. Interaction of dimeric sPSGL-1 with sP-selectin resulted in 10−13% enhancement of the intrinsic protein fluorescence of sP-selectin. This increase in fluorescence is either due to changes in protein conformation caused by ligand binding or by perturbation of the environment of one or more tryptophan residues in P-selectin by sPSGL-1 itself.

The intrinsic fluorescence enhancement of P-selectin upon binding to PSGL-1 was used to monitor the formation of the receptor−ligand complex. By this method we analyzed the interaction between sP-selectin and both fucosyl isoforms of dimeric sPSGL-1 under equilibrium conditions. In these experiments, sPSGL-1/Fuc-TIII and Fuc-TVII bound to sP-selectin with dissociation constants of 3 nM and 80 nM, respectively. We hypothesize that the differences in affinity between these isoforms stem from variations in their fucosylation patterns as suggested by their different migration on SDS−PAGE. Because fucosyltransferase VII is the dominant fucosyltransferase in myeloid cells, it is likely that the sPSGL-1/Fuc-TVII variant most closely mimics wild-type PSGL-1, although we cannot be certain that our recombinant and wild-type PSGL-1 have identical affinities for P-selectin (*17*). This issue needs to be revisited when adequate amounts of leukocyte PSGL-1 become available. The K_d for the sPSGL-1/Fuc-TVII interaction with sP-selectin in our fluorescent studies (80 nM) was similar to the apparent K_d determined for sP-selectin binding to the surface of HL60 cells (70 nM) (*28*). This similarity may arise from the fact that the high-affinity binding sites on HL-60 cells may not be present at a density sufficient to induce cooperative binding effects. Alternately, the combination of several high-affinity clustered sites may combine with lower affinity individual sites to give an apparent cellular affinity similar to that of the actual K_d for the two proteins in solution.

In summary, we have examined the interaction of P-selectin and PSGL-1 in a simple soluble system that eliminates the effects of ligand density and cell surface clustering on receptor−ligand binding. These binding data were fit to a simple bimolecular model and the binding affinity and stoichiometry of binding were determined. Using this system, we have shown that sP-selectin and sPSGL-1 interact with high affinity and that the affinity may in part be affected by the fucosylation pattern of PSGL-1. This is the first determination of the binding constant, K_d, for P-selectin and PSGL-1 in a cell-free system. The dissociation constants determined by these experiments will facilitate the modeling of selectin−ligand interactions in more complex systems and will lead to a better understanding of the molecular dynamics of vascular cell adhesion under conditions of flow.

ACKNOWLEDGMENT

We thank Genetics Institute for the generous gift of pure soluble PSGL-1 and Dr. Gary Gilbert for helpful discussions.

REFERENCES

1. Butcher, E. C. (1991) *Cell 67*, 1033−6.
2. Lawrence, M. B., and Springer, T. A. (1991) *Cell 65*, 859−73.
3. Frenette, P. S., and Wagner, D. D. (1996) *New Engl. J. Med. 334*, 1526−9.
4. Frenette, P. S., and Wagner, D. D. (1996) *New Engl. J. Med. 335*, 43−5.
5. Mayadas, T. N., Johnson, R. C., Rayburn, H., Hynes, R. O., and Wagner, D. D. (1993) *Cell 74*, 541−54.
6. Johnston, G. I., Cook, R. G., and McEver, R. P. (1989) *Cell 56*, 1033−44.
7. Kansas, G. S. (1996) *Blood 88*, 3259−87.
8. Berman, C. L., Yeo, E. L., Wencel-Drake, J. D., Furie, B. C., Ginsberg, M. H., and Furie, B. (1986) *J. Clin. Invest. 78*, 130−7.
9. Bonfanti, R., Furie, B. C., Furie, B., and Wagner, D. D. (1989) *Blood 73*, 1109−12.
10. Stenberg, P. E., McEver, R. P., Shuman, M. A., Jacques, Y. V., and Bainton, D. F. (1985) *J. Cell Biol. 101*, 880−6.
11. Geng, J. G., Bevilacqua, M. P., Moore, K. L., McIntyre, T. M., Prescott, S. M., Kim, J. M., Bliss, G. A., Zimmerman, G. A., and McEver, R. P. (1990) *Nature 343*, 757−60.
12. Larsen, E., Celi, A., Gilbert, G. E., Furie, B. C., Erban, J. K., Bonfanti, R., Wagner, D. D., and Furie, B. (1989) *Cell 59*, 305−12.
13. Sako, D., Chang, X. J., Barone, K. M., Vachino, G., White, H. M., Shaw, G., Veldman, G. M., Bean, K. M., Ahern, T. J., Furie, B., Cumming, D. A., and Larsen, G. R. (1993) *Cell 75*, 1179−86.
14. Geng, J. G., Moore, K. L., Johnson, A. E., and McEver, R. P. (1991) *J. Biol. Chem. 266*, 22313−8.
15. Varki, A. (1997) *J. Clin. Invest. 100*, S31−5.
16. Moore, K. L., Stults, N. L., Diaz, S., Smith, D. F., Cummings, R. D., Varki, A., and McEver, R. P. (1992) *J. Cell Biol. 118*, 445−56.
17. Maly, P., Thall, A., Petryniak, B., Rogers, C. E., Smith, P. L., Marks, R. M., Kelly, R. J., Gersten, K. M., Cheng, G., Saunders, T. L., Camper, S. A., Camphausen, R. T., Sullivan, F. X., Isogai, Y., Hindsgaul, O., von Andrian, U. H., and Lowe, J. B. (1996) *Cell 86*, 643−53.
18. Larsen, E., Palabrica, T., Sajer, S., Gilbert, G. E., Wagner, D. D., Furie, B. C., and Furie, B. (1990) *Cell 63*, 467−74.
19. Sako, D., Comess, K. M., Barone, K. M., Camphausen, R. T., Cumming, D. A., and Shaw, G. D. (1995) *Cell 83*, 323−31.
20. Pouyani, T., and Seed, B. (1995) *Cell 83*, 333−43.
21. Wilkins, P. P., Moore, K. L., McEver, R. P., and Cummings, R. D. (1995) *J. Biol. Chem. 270*, 22677−80.
22. Snapp, K. R., Ding, H., Atkins, K., Warnke, R., Luscinskas, F. W., and Kansas, G. S. (1998) *Blood 91*, 154−64.
23. Gibson, R. M., Kansas, G. S., Tedder, T. F., Furie, B., and Furie, B. C. (1995) *Blood 85*, 151−8.
24. Bruinsma, R. (1997) *Proc. Natl. Acad. Sci. U.S.A. 94*, 375−6.
25. Konstantopoulos, K., Kukreti, S., Smith, C. W., and McIntire, L. V. (1997) *J. Leukocyte Biol. 61*, 179−87.
26. Dembo, M., Torney, D. C., Saxman, K., and Hammer, D. (1988) *Proc. R. Soc. London, Ser. B: Biol. Sci. 234*, 55−83.
27. Alon, R., Hammer, D. A., and Springer, T. A. (1995) *Nature 374*, 539−42.
28. Ushiyama, S., Laue, T. M., Moore, K. L., Erickson, H. P., and McEver, R. P. (1993) *J. Biol. Chem. 268*, 15229−37.
29. Ruegg, U. T. (1977) *Methods Enzymol 47*, 123−6.
30. Gilbert, G. E., Furie, B. C., and Furie, B. (1990) *J. Biol. Chem. 265*, 815−22.
31. Fujimoto, T. T., Noda, M., Takafuta, T., Shimomura, T., Fujimura, K., and Kuramoto, A. (1996) *Int. J. Hematol. 64*, 231−9.
32. Winzor, D. J., and Sawyer, W. H. (1995) *Quantitative Characterization of Ligand Binding*, 1st ed., Wiley-Liss, New York.
33. Bell, G. I. (1978) *Science 200*, 618−27.
34. Tedder, T. F., Steeber, D. A., Chen, A., and Engel, P. (1995) *FASEB J. 9*, 866−73.
35. Springer, T. A. (1994) *Cell 76*, 301−14.
36. Borges, E., Pendl, G., Eytner, R., Steegmaier, M., Zollner, O., and Vestweber, D. (1997) *J. Biol. Chem. 272*, 28786−92.
37. Borges, E., Tietz, W., Steegmaier, M., Moll, T., Hallmann, R., Hamann, A., and Vestweber, D. (1997) *J. Exp. Med. 185*, 573−8.
38. Borges, E., Eytner, R., Moll, T., Steegmaier, M., Campbell, M. A., Ley, K., Mossmann, H., and Vestweber, D. (1997) *Blood 90*, 1934−42.
39. Norman, K. E., Moore, K. L., McEver, R. P., and Ley, K. (1995) *Blood 86*, 4417−21.
40. Takada, M., Nadeau, K. C., Shaw, G. D., Marquette, K. A., and Tilney, N. L. (1997) *J. Clin. Invest. 99*, 2682−90.

41. Mehta, P., Patel, K. D., Laue, T. M., Erickson, H. P., and McEver, R. P. (1997) *Blood 90*, 2381−9.
42. Wilkins, P. P., McEver, R. P., and Cummings, R. D. (1996) *J. Biol. Chem. 271*, 18732−42.
43. Li, F., Wilkins, P. P., Crawley, S., Weinstein, J., Cummings, R. D., and McEver, R. P. (1996) *J. Biol. Chem. 271*, 3255−64.
44. Niemela, R., Natunen, J., Majuri, M. L., Maaheimo, H., Helin, J., Lowe, J. B., Renkonen, O., and Renkonen, R. (1998) *J. Biol. Chem. 273*, 4021−6.
45. Knibbs, R. N., Craig, R. A., Natsuka, S., Chang, A., Cameron, M., Lowe, J. B., and Stoolman, L. M. (1996) *J. Cell Biol. 133*, 911−20.
46. Kimura, H., Shinya, N., Nishihara, S., Kaneko, M., Irimura, T., and Narimatsu, H. (1997) *Biochem. Biophys. Res. Commun. 237*, 131−7.
47. Snapp, K. R., Craig, R., Herron, M., Nelson, R. D., Stoolman, L. M., and Kansas, G. S. (1998) *J. Cell. Biol. 142*, 263−70.

BI981341G